Regulation of Sodium-dependent Phosphate Transport in Osteoclasts

Anandarup Gupta, Xiao-Li Guo, Ulises M. Alvarez, and Keith A. Hruska

Renal Division, Barnes-Jewish Hospital of St. Louis, Washington University School of Medicine, St. Louis, Missouri 63110

Abstract

Osteoclasts are the primary cells responsible for bone resorption. They are exposed to high ambient concentrations of inorganic phosphate (Pi) during the process of bone resorption and they possess specific Pi-transport system(s) capable of taking up Pi released by bone resorption. By immunochemical studies and PCR, we confirmed previous studies suggesting the presence of an Na-dependent Pi transporter related to the renal tubular "NaPi" proteins in the osteoclast. Using polyclonal antibodies to NaPi-2 (the rat variant), an $\sim$ 95-kD protein was detected, localized in discrete vesicles in unpolarized osteoclasts cultured on glass coverslips. However, in polarized osteoclasts cultured on bone, immunofluorescence studies demonstrated the protein to be localized exclusively on the basolateral membrane, where it colocalizes with an Na-H exchanger but opposite to localization of the vacuolar H-ATPase. An inhibitor of phosphatidylinositol 3-kinase, wortmannin, and an inhibitor of actin cytoskeletal organization, cytochalasin D, blocked the bone-stimulated increase in Pi uptake. Phosphonoformic acid (PFA), an inhibitor of the renal NaPi-cotransporter, reduced NaPi uptake in the osteoclast. PFA also elicited a dose-dependent inhibition of bone resorption. PFA limited ATP production in osteoclasts attached to bone particles. Our results suggest that Pi transport in the osteoclast is a process critical to the resorption of bone through provision of necessary energy substrates. (*J. Clin. Invest.* 1997. 100: 538–549.) Key words: osteoclasts • Na-dependent phosphate cotransporter • phosphatidylinositol 3-kinase • phosphonoformic acid • bone resorption

Introduction

Phosphate is the basic anionic component of the mineralized bone matrix. Osteoblasts are responsible for phosphate deposition in bone, whereas osteoclasts (OCs)[1] are involved in resorption of the mineral and matrix components of bone (1). Bone mineral is primarily hydroxyapatite, $Ca_3(PO_4)_2Ca(OH)_2$, an alkaline salt, and hence its dissolution requires protonation, furnished by the proton-ATPase (H-ATPase) on the ruffled membrane of the OC (2). As a result of resorption, OCs are exposed to high ambient concentrations of inorganic phosphate (Pi) from the dissolution of bone mineral. Therefore, to meet the rather immense energy requirements of the OC during the cyclical processes of migration, attachment, and resorption, these cells may possess specific transport mechanisms related to Pi utilization and ATP production. The OC maintains a high demand for ATP (1, 3) even when it is not secreting protons, due in part to the energy demands of motility.

Several renal Na-dependent phosphate-cotransporters (NaPi) have been cloned and characterized from the rabbit and other species using the *Xenopus oocyte* expression cloning system (4–7). Variants of the renal NaPi have been assigned numbers on the basis of species, i.e., NaPi-1 and NaPi-6 in the rabbit, NaPi-2 in the rat, NaPi-3 in the human renal cortex, NaPi-4 in the opossum kidney cell, NaPi-5 in the flounder, and NaPi-7 in the mouse. Based upon overall identity of the variants, the NaPis have been grouped into either type I (NaPi-1) or type II (NaPi-2 to-7) families. Polyclonal antibodies have been raised against synthetic NH_2- and COOH-terminal peptides of NaPi-2 which has permitted immunochemical detection of the variants of the NaPis across species (8). While the type I and II NaPis are expressed mainly in the kidney, a third family of NaPi (type III) has been described recently (9). The cell surface receptors for gibbon ape leukemia virus (Glvr-1, Pit-1) and rat amphotropic virus (Ram-1, Pit-2) were demonstrated to serve normal cellular functions as NaPis. In contrast to the type I and II families, both Pit-1 and -2 are widely distributed, in addition to their presence in the kidney. The highest expressions are in the liver, lung, striated muscle, heart, brain, and bone marrow. Osteoblasts have been shown to express the type III family of NaPis.

We have previously reported preliminary observations characterizing Na-dependent Pi transport in the OC (10). We reported cross-reactivity between a protein in OC lysates and in membrane fractions and an antipeptide antibody to an NH_2-terminal segment of NaPi-2. Immunolocalization studies revealed that the OC anti–NaPi-2 immunoreactive protein was located largely in a cytosolic vesicular compartment in cells cultured on glass; but upon attachment to bone, plasma membrane expression increased noticeably in the plasma membrane not in contact with bone. In this study, we provide additional evidence for an NaPi-2–like protein in the OC with a significantly larger apparent molecular size than the rodent kidney protein, and present initial studies suggesting a mechanism of NaPi-2–containing vesicular traffic to the plasma membrane in the presence of bone. Most importantly, we demonstrate that a specific inhibitor of the renal NaPi-2 protein also inhibits OC Na-dependent Pi transport, and by so doing decreases bone resorption. We hypothesize that upon attachment to bone the polarization of the OC is associated with redistribution of the NaPis from discrete vesicular pools into the baso-

1. *Abbreviations used in this paper:* BS, blocking solution; GLUT4, basal plasma membrane glucose transporter; H-ATPase, protein-ATPase; NaPi, Na-dependent phosphate cotransporter; NHE-1, Na-H exchanger isoform 1; OC, osteoclast; PFA, phosphonoformic acid; Pi, inorganic phosphate; PI 3-K, phosphatidylinositol 3-kinase; *xz*, cross section.

lateral plasma membrane, and that Pi transport is critical for bone resorption.

Methods

Materials

Phosphonoformic acid (PFA), colchicine, wortmannin, Ricin-TRITC, and other fluorescent-conjugated antibodies were purchased from Sigma Chemical Co. (St. Louis, MO). The [^{3}H]-proline-labeled rat bone chips used in bone resorption assays were provided by Dr. S.L. Teitelbaum (Department of Pathology, Washington University School of Medicine, St. Louis, MO). The polyclonal antibodies to either the NH$_2$ terminus of NaPi-2 (MMSYSERLGGPAV) or the COOH terminus of NaPi-2 (LALPAHHNATRL) were provided by Dr. Heini Murer and Dr. Jürg Biber (Institute of Physiology, University of Zurich, Zurich, Switzerland). The monoclonal antibody E11 directed toward the 31-kD subunit of vacuolar H-ATPase was used as ascites fluid provided by Dr. S.L. Gluck (Renal Division, Washington University School of Medicine, St. Louis, MO). The monoclonal antibody to Na-H exchanger isoform 1 (NHE-1) was provided by Dr. D. Biemesderfer (Department of Nephrology, Yale University School of Medicine, New Haven, CT). K$_2$H^{32}PO$_4$ was obtained from ICN Biomedicals Inc. (Costa Mesa, CA). The rabbit OC cDNA library was a kind gift of Dr. M. Kumagawa (Sakado, Japan). Dentine slices were used for the immunofluorescent experiments. Both endoglycosidase H (endo-β-*N*-acetylglucosaminidase H) and *N*-glycosidase F were purchased from Boehringer Mannheim (Indianapolis, IN). All other reagents were of analytical grade quality and were purchased from Sigma Chemical Co.

OC cell culture

Avian OCs. Avian bone marrow macrophage precursors which differentiate into OCs were isolated from calcium-deprived hens and cultured as previously described (11). Briefly, laying hens were maintained on a calcium-free diet (Ralston Purina Co., St. Louis, MO) for 3 to 4 wk, at which time bone marrow was harvested. Mononuclear cells were isolated by Ficoll-Hypaque gradient centrifugation (Litton Bionetics, Rockville, MD) and the cells adherent at 24 h were cultured at $2.5 \times 10^7/25$ cm^2 in α-MEM plus 5% FCS plus 5% chicken serum, 100 μg/ml streptomycin, 100 IU/ml penicillin, and 3 μg/ml cytosine 1β-D arabino furanoside. Temperature was maintained at 39°C in a water-saturated atmosphere containing 10% CO$_2$. Under these conditions, the cells (OC precursors) fused within 3–5 d forming an 85–95% pure population of multinucleated cells. The cells were characterized as having an OC phenotype by a variety of functional, morphological, and immunohistochemical criteria. Functionally, the OC precursors differentiated in culture and formed resorption pits when added to bone slices. Morphologically, they expressed ruffled borders upon attachment to bone and were uniformly TRAP (tartrate resistant acid phosphatase) positive. They expressed several OC-specific antigens detected by monoclonal antibodies. Therefore, the multinucleated OCs were formed in culture and not directly isolated from bone.

Rabbit OCs. Unfractionated bone cells were isolated from long bones of 7-d-old rabbits, as previously described (12). The bone cells were disaggregated in αMEM; bone particles were removed by sedimentation under normal gravity. Cells were suspended in αMEM supplemented with 10% FCS and seeded into culture plates. After 3 h of culture, the medium was exchanged for fresh medium and after an additional 21 h of culture, the cells were washed with PBS to remove nonadherent cells. Subsequently, the cells were washed with PBS plus 0.001% Pronase E plus 0.02% EDTA for 10 min at 37°C. The stromal cells were removed by washing several times and the remaining cells comprised ∼ 95% pure OCs, positive for TRAP activity (13).

Mouse OCs. The tibiae and femurs of 7-wk-old mice were used to isolate bone cells, as previously described (13). The cells were suspended in αMEM and cultured at 37°C in a 5% CO$_2$ incubator. M-CSF-1 was added to the cultures at a concentration of 1,000 U/ml

and the nonadherent cells were removed after 24 h. The cells were suspended in a Ficoll-Hypaque gradient (Litton Bionetics) and the interface removed and suspended in αMEM. ST-2 stromal cells were added at a seeding density ratio of 1:10 in the presence of dexamethasone (10 μM), 1,25(OH)$_2$D$_3$ (10 nM), and M-CSF-1. The cultures were maintained for 10 to 12 d; subsequently, the stromal cells were removed by collagenase treatment. The remaining adherent cells were pure mouse OCs, as previously described (13).

Pi transport studies

Avian OCs were plated in 24-well dishes and washed with the incubation buffer which contained (mM): 150 NaCl (or choline chloride), 5 KCl, 1.8 MgSO$_4$, 1 CaCl$_2$, 10 Hepes, 0.1 K$_2$H^{32}PO$_4$, and 5 glucose at pH 7.4. 1 ml of Pi uptake assay buffer (^{32}Pi, 1 μCi/ml) was added to the incubation buffer for varying periods of time at room temperature. After the specified time intervals, the cells were washed with ice-cold incubation buffer followed by solubilization in 0.2 N NaOH. Pi uptake was determined by liquid scintillation counting. Protein contents were determined for each time point for normalization of the counts (cpm) obtained from Pi uptake studies. The raw data (in cpm) were transformed (to μmol of Pi) and presented as μmol/mg protein, as previously described (10).

Western blot analysis

Chicken OCs were used on day 5 in culture for preparation of crude membrane fractions. The cells were first washed twice with PBS and then lysed in homogenization buffer which contained (mM): 15 Tris, pH 7.5, 0.25 sucrose, 2.5 MgCl$_2$, and 2.5 EGTA. Briefly, the cells were homogenized using a Dounce homogenizer, and then the homogenate was centrifuged at 10,000 rpm for 10 min in a rotor (Sorvall SS-34; DuPont Co., Wilmington, DE). The supernatant was collected and ultracentrifuged at 40,000 rpm in a rotor (Ti 70.1; Beckman Instruments, Schaumburg, IL) for 1 h at 4°C. The pellet containing the membrane fractions was solubilized in sample buffer containing 2% SDS, as previously described (14). The protein contents were determined using the BCA protein assay (Pierce Chemical Co., Rockford, IL) and equal amounts of proteins were loaded per lane (100 μg), and were analyzed by SDS-PAGE on 8% gels. The gel was then electroblotted onto a PVDF membrane (Millipore, Bedford, MA) by wet-dry transfer (Enprotech; Integrated Separation Systems, Natick, MA). Nonspecific protein binding was blocked with 5% nonfat dry milk powder dissolved in PBS containing 0.1% Tween 20. The blots were incubated overnight with a 1:1,000 dilution of the primary antibodies to NaPi-2 (NH$_2$ or COOH terminus). This was followed by detection with a horseradish peroxidase–conjugated secondary goat anti–rabbit antibody (Sigma Chemical Co.; 1:1,000 dilution). The secondary antibody (horseradish peroxidase–conjugated goat anti–rabbit antibody) was detected by the enhanced chemiluminescence detection kit (Amersham Corp., Arlington Heights, IL) following the manufacturer's instructions. In those experiments where (surface) biotinylated membranes were used, intact chicken OCs were first washed twice with PBS supplemented with CaCl$_2$ (0.1 mM) and MgCl$_2$ (1.0 mM). The OCs were labeled for 30–60 min at 4°C with 0.5 mg/ml sulfo-NHS-LC-biotin (i.e., the water soluble *N*-hydroxysuccinimide long chain ester of biotin; Pierce Chemical Co.) freshly diluted into biotinylation buffer which consisted of PBS with 1 mM EDTA. The cells were then washed twice for 20 min at 4°C with ice-cold PBS containing 5 mM glycine to quench the unreacted biotin. After two more rinses with PBS, the cells were solubilized on ice with lysis buffer containing (mM): 150 NaCl, 20 Tris, 2 mM EDTA, and 0.5% NP-40, at pH 7.4. After determination of protein content, the lysates were incubated with avidin agarose (Pierce Chemical Co.). The avidin–agarose immunoprecipitates were washed three times with lysis buffer and twice with 20 mM Tris-HCl, pH 7.5. The samples were then solubilized in Laemmli sample buffer and boiled for 15 min to dissociate the avidin–biotin complex. The biotinylated proteins were separated on an 8% SDS-PAGE. Thereafter, standard immunoblotting techniques were used, as described above.

Immunostaining

Avian OCs were plated in 4-well Lab-Tek (Nunc Inc., Naperville, IL) culture chambers and cells were used on day 5 of culture when most cells were mature multinucleated OCs, as previously described (14). Rabbit OCs were studied on day 3 of culture. The cells were briefly rinsed twice in ice-cold PBS and then fixed and permeabilized with 100% methanol at −80°C. The cells were blocked with blocking solution (BS) which comprised PBS containing 20% goat serum and 1% polyethylene glycol for 1–2 h. The cells were incubated overnight in a 1:500 dilution of the various primary antibodies at 4°C in the BS described above. After two 15-min rinses with PBS with 0.1% Tween 20, the cells were further incubated with FITC-conjugated goat anti–rabbit antibodies in BS for 2 h. The cells were washed with PBS and then mounted with VectaShield™ (Vector Laboratories, Inc., Burlingame, CA). Negative controls were performed with nonimmune rabbit sera in the BS formulation described above. Double-label immunofluorescence microscopy was performed using a confocal laser scanning microscope (Carl Zeiss, Inc., Thornwood, NY). Briefly, photomicrographs were obtained with a scanning laser confocal microscope system (LSM 410; Carl Zeiss, Inc.). The system consisted of an inverted microscope (135 Axiovert; Carl Zeiss, Inc.) fitted with an Omnicron argon/krypton laser for confocal excitation. Samples were viewed with a 63×/1.25 n.a. oil objective, and images were recorded in a 512 × 512 pixel format. FITC images were recorded using the 488 nm argon excitation line, whereas the Texas red images were recorded with the 568 argon excitation line. The data were collected as emission intensities using barrier filters for FITC (515–540 nm bandpass) and Texas red (590–640 nm bandpass). Data processing was accomplished with the LSM 410 software package (Carl Zeiss, Inc.). Photomicrographs were produced from a color video printer (Mavigraph; Sony Corp., Park Ridge, NJ) or stored in TIF image format for post processing, as previously described (10, 14).

PCR of rabbit OC DNA

A sequence of the rabbit osteoclastic NaPi-6 was amplified by PCR from a randomly primed ZapII cDNA library generated from rabbit OCs (12). Primers for the NaPi were synthesized from two regions highly conserved among the NaPi-2 and NaPi-6 species isoforms (5): sense primer 5'CCACCATGGAGAAATGCAA (1063–1081 from NaPi-6) and antisense primer 5'CCCGAGATGTTGAAGAAGAAGTG (1500–1522 from NaPi-6). Amplifications were carried out with standard methods using 5 μl of the amplified library (10^{10} plaque forming units/ml) as template. Reactions were denatured at 94°C for 0.5 min, annealed at 49°C for 1 min, and elongated at 72°C for 3 min with a total of 35 cycles (15). The expected size product (460 bp) was obtained from both sets of primers and ligated with PCRII vector (Invitrogen Corp., San Diego, CA). Sequences were determined from both ends from individual clones using the dideoxynucleotide chain termination method of Sanger et al. (16).

Bone resorption assay

[³H]Proline-prelabeled bone release. Chicken and mouse OCs were cultured in the presence of bone chips for 5 d in 24-well plates. On day 1 of the experiments, [³H]proline-prelabeled devitalized rat bone chips (2.5×10^5 cpm/well) were added. On day 3, PFA was added at the individual concentrations of 1, 2, and 5 mM to each well. 1.0 ml of the culture media was sampled on both days 4 and 5 to assess the amount of ³H-bone being resorbed. After the last sampling period, the cells were lysed with 0.2 N NaOH and assayed for protein content. Bone resorption was represented by cpm [³H]proline/mg protein, and as percentage of control.

Pit assay. Chicken OC precursors were allowed to differentiate on osteologic discs (Millenium Biologix Inc., Kingston, Ontario, Canada) coated with a 1-μm-thick calcium phosphate film. On day 3 of culture, PFA was added at the individual concentrations of 1, 2, and 5 mM to each well. After 48 h in culture, on day 5, the discs were washed with bleach to remove all adherent OCs. The discs were then washed in water and allowed to air dry before they were examined for bone resorption, as previously described (17).

Adenosine-5'-triphosphate (ATP) assay

Chicken OC precursors were allowed to differentiate into multinucleated OCs for 4 d in 24-well plates. On day 4, parallel sets of cultures were incubated with 1, 2, and 5 mM PFA in the absence and presence of [³H]proline-prelabeled devitalized rat bone chips (2.5×10^5 cpm/well). After 48 h in culture, the OCs were processed for assay of total ATP content according to methods described by Adams (18), and following the manufacturer's instructions (Sigma Chemical Co., St. Louis, MO). In the described procedure, phosphoglycerate phosphokinase is used to catalyze the reaction: ATP + 3-phosphoglycerate → ADP + 1,3-diphosphoglycerate; the enzyme glyceraldehyde phosphate dehydrogenase is also present in the reaction mixture to catalyze the following: 1,3-diphosphoglycerate + NADH → glyceraldehyde-3-P + NAD + P. By determining the decrease in absorbance at 340 nm that results when NADH is oxidized to NAD, a measure of the amount of ATP originally present is obtained. Briefly, the cells were washed twice with ice-cold PBS before lysis in 2 ml of lysis buffer containing (mM): 150 NaCl, 20 Tris, 2 mM EDTA, and 0.5% NP-40, pH 7.4. After lysis, 1 ml of the OC lysate was added to 1 ml of 12% TCA on ice for 10 min to precipitate the proteins in the cell lysates. The samples were then centrifuged at 3,000 rpm for 10 min to obtain a clear supernatant. The reaction mixture comprised 1.0 ml of a buffered solution of 3-phosphoglyceric acid, 0.5 ml of the supernatant, 0.3 mg NADH, and 1.5 ml H_2O (total volume: 3 ml). The initial absorbance of this reaction mixture was recorded at 340 nm. Subsequently, 40 μl of glyceraldehyde phosphate dehydrogenase/phosphoglycerate phosphokinase (800 and 450 U/ml, respectively) enzyme mixture was added to the reaction mixture and the final minimum absorbance (at 340 nm) was recorded. Thereafter, the absorbance readings were converted to nmol ATP/μg protein after determination of protein content and, subsequently converted to percentage of control for presentation.

Statistics

The statistical computation for the "bone resorption" assay was done as follows: the raw data points (³H-cpm/ml) for the bone resorption assay were used to obtain the mean for the (untreated) control group. Each raw data point within that group was divided by the mean and subsequently transformed (multiplying the quotient by 100) to get percentage of control for each data point within that group. From these transformed data points, we determined the mean±SEM for the control group. To obtain similar data for the experimental treatment groups, each raw data point was divided by the original mean of control group; the quotients were similarly transformed into percentage of control. Therefore, similar to that for the control group, means± SEM were obtained for the experimental groups. For all other experiments, statistical comparisons were performed on means±SEM and differences between means were considered significant at $P < 0.01$, using the Student's *t* test.

Results

Immunochemical characterization of the NaPi. We have extended our preliminary characterization of the immunochemical identity of the NaPi in the OC (10) which was based on the detection of an OC protein by an NH_2-terminal antipeptide NaPi-2 antibody (8). Since the protein detected was larger than the expected size from the renal tubule NaPi-2, it was critical to obtain further evidence that the detected protein was in fact NaPi-related. We performed peptide competition studies and used a second antibody directed against the COOH terminus of the NaPi-2 molecule. As shown in Fig. 1, both the NH_2- and COOH-terminal antipeptide antibodies detected proteins of the same molecular size, and peptide competition studies using the respective NaPi-2 NH_2 terminus peptide completely
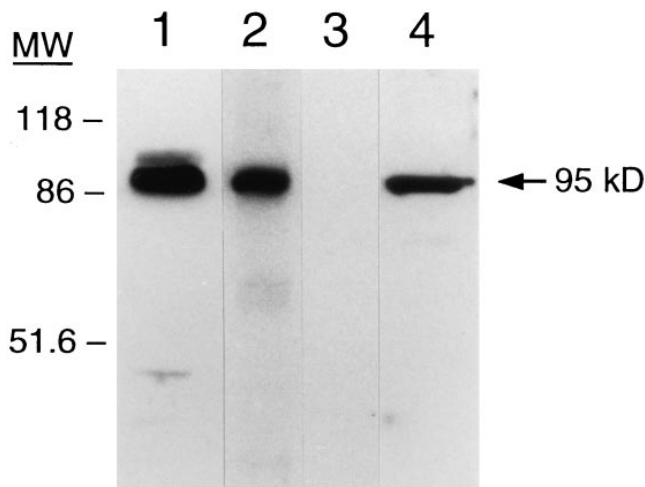
Figure 1. Detection of NaPi in avian OCs. Membrane fractions and total cell lysates prepared from avian OCs were separated on an 8% SDS-PAGE for immunoblotting with NaPi-2 antibodies. Lane *1*: immunoblot of biotinylated plasma membranes with an antibody toward the NH_2 terminus of NaPi-2. The apparent molecular mass of the detectable band in lane *1* is $\sim$ 95 kD. Lane *2*: immunoblot of total OC lysates with the NH_2-terminal antibody for NaPi-2. Lane *3*: specificity of the band detected in lane *2* was demonstrated by preincubation of the NH_2-terminal antibody with 100 μg/ml of the NH_2-terminal synthetic peptide. Lane *4*: immunoblot of total OC lysates with an antibody toward the COOH terminus of NaPi-2.

blocked detection of the protein. A 95-kD band was detected in chicken microsomal fractions (lane *1*) and in whole cell lysates (lane *2*) by the NH_2-terminal antibody. We have reported previously that a protein of the same molecular size was detected in rabbit OC lysates by the NH_2-terminal antibody (10). The NaPi-2–like protein detected in total chicken OC lysates with an antibody toward the COOH terminus of NaPi-2 is shown in lane *4*. Since there is 100% amino acid identity at the COOH terminus of NaPi-2, -3, -4, and -6 (LALPAHH-NATRL, 5), this provides further evidence that the OC protein is of the NaPi-2 family. In data not shown, we found that the NaPi-2–related proteins of the OC were not N-glycosylated, by the lack of susceptibility of the 95-kD band to either endoglycosidase H or PNGase F, in contrast to that of NaPi-2 (19).
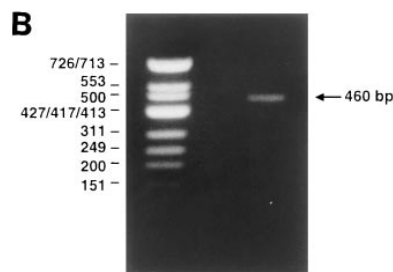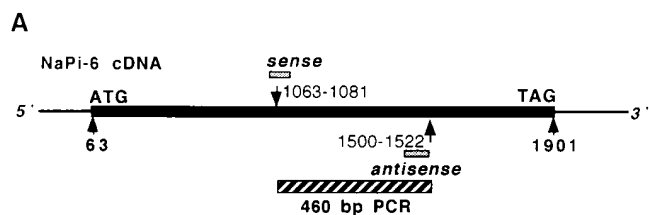
Detection of an NaPi-2–related gene in the rabbit OC. We wished to determine whether an NaPi-2–related protein was present in the OC. Since the species variants of the NaPi (4–7), especially NaPi-2 to -6, share several conserved domains, we performed PCR using primers flanking a conserved region among NaPi-2 and -6 (rabbit) and a rabbit OC cDNA library (Fig. 2 *A*). A 460-bp PCR product of identical sequence to NaPi-6 (5) was obtained (Fig. 2 *B*). As a result of the immunologic cross-reactivity of the two NaPi-2 antibodies to rabbit and avian proteins of the same size, and the presence of a NaPi-6–related cDNA in the OC, we conclude that the 95-kD protein is likely a NaPi-related protein. Since the avian NaPi protein has probably not been cloned, the corresponding PCR product from the avian OC is not shown.

Cellular distribution of the NaPi in unpolarized OCs. Using immunoblots of microsomal fractions isolated from chicken OCs grown either in the presence or absence of bone in our preliminary studies, we reported that the stimulatory effect of bone particles on Pi uptake by OCs was accompanied by an increased level of expression of the NaPi in cellular membranes (10). This occurred without a change in the amount of NaPi protein in total cell lysates in agreement with the inability of actinomycin D or cycloheximide to block the increase in Na dependent Pi transport induced by the presence of bone, as previously reported (10).

Preliminary immunolocalization studies of the OC NaPi-2–like protein using laser scanning confocal microscopy to examine the cellular distribution of the NaPi in OCs grown on glass revealed staining of a vesicular, possibly endosomal, compartment distributed diffusely throughout the cell. As shown in Fig. 3, when using the COOH-terminal antibody against NaPi-2, a similar distribution of vesicular staining was detected in OCs cultured on glass.

To further characterize the endosomal distribution of the OC NaPi, ricin was used as an endocytic marker. Ricin is a 60-kD lectin which binds to galactose residues of membrane glycoproteins and glycolipids and thereby acts as a probe for membrane traffic (20). Ricin is widely used as a common marker for apical recycling endosomes and recycling of apically internalized membrane proteins in polarized epithelial cells. The majority of apically internalized ricin recycles back to the apical plasma membrane, while a small percentage is transcytosed to the basolateral plasma membrane or transported to the lysosomes and the Golgi complex (20). We hypothesized that an OC endosomal fraction containing the NaPi would redistribute when the OC polarized in response to bone. OCs were treated with TRITC-conjugated ricin for 15 min at 37°C. The cells were then fixed and processed for immunostaining with the NaPi-2 antibody. Fig. 4 *A* shows an OC cul-

A

NaPi-6 cDNA

sense
1063-1081

ATG   TAG
5'   3'
63
1500-1522   1901
antisense
460 bp PCR

B

726/713 —
553 —
500 —
427/417/413 —
311 —
249 —
200 —
151 —

← 460 bp

Figure 2. PCR of NaPi in rabbit OC. (*A*) A map of the NaPi-6 cDNA demonstrates the regions from which NaPi-6 cDNA primers for the PCR reactions were derived. (*B*) PCR of rabbit OC mRNA. An expected 460-bp fragment was detected. The sequence of the PCR fragment was identical to NaPi-6 in the rabbit kidney.
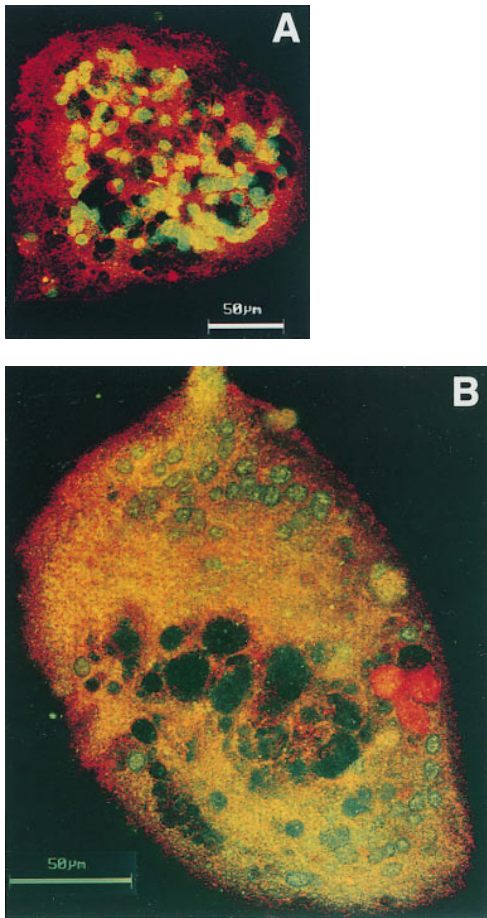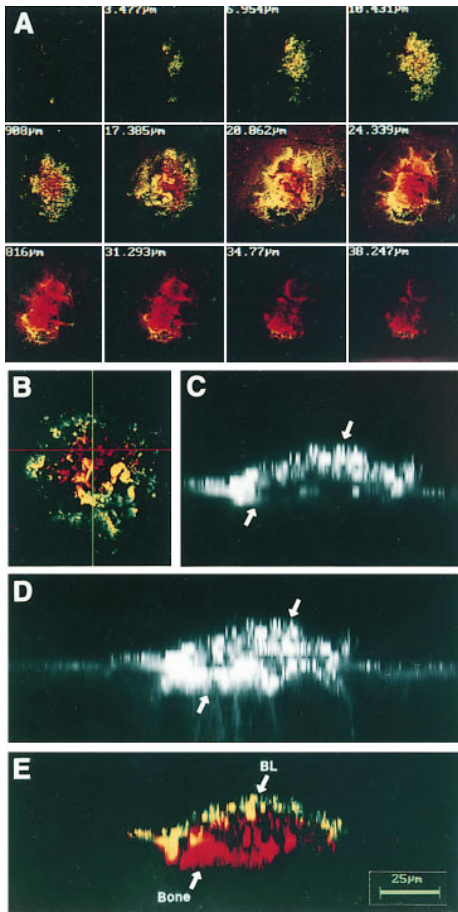
Figure 3. Immunofluorescent localization of NaPi in the avian OC using laser scanning confocal microscopy. Avian OCs were cultured on glass coverslips and immunostained with antibodies to NaPi-2 (NH$_2$ and COOH termini). (*A*) An apical (i.e., close to the glass surface) image of an OC; the color red represents the reflection image of the OC whereas the punctate green staining represents the immunofluorescence obtained with the NH$_2$-terminal NaPi-2 antibody. (*B*) Apical image of an OC; the color red represents the reflection image of the OC whereas the punctate green staining represents the immunofluorescence obtained with the COOH-terminal NaPi-2 antibody.
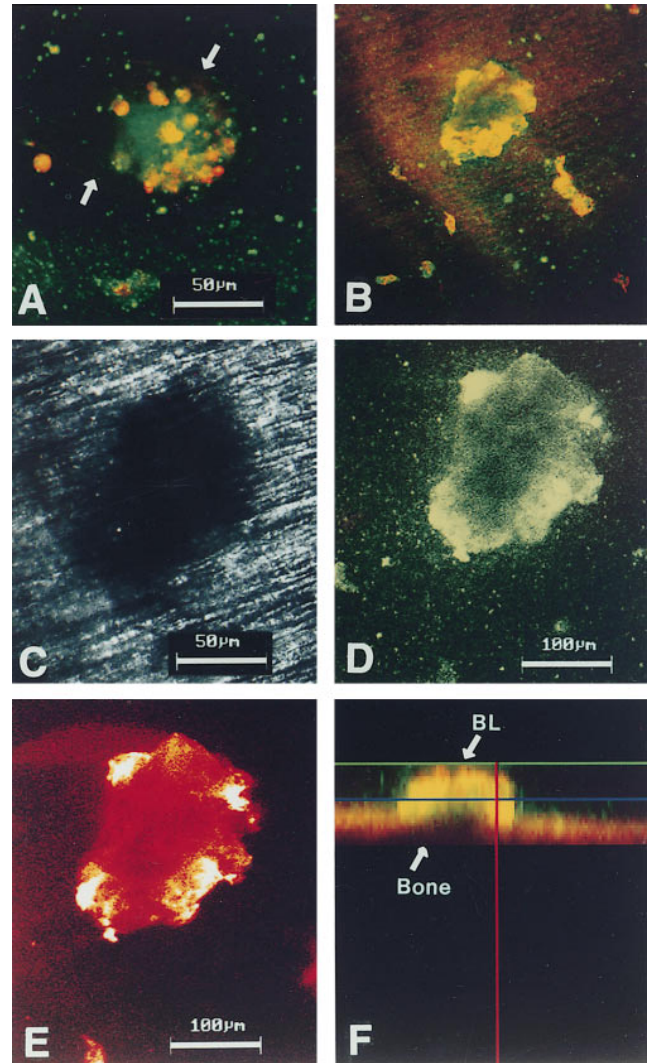
Figure 4. Localization of NaPi-2 protein in endosomes in avian OCs using laser scanning confocal microscopy. (*A*) Avian OCs cultured on glass and double-stained with both TRITC-conjugated ricin and the NaPi-2 antibody (NH$_2$ terminus). (*B*) Avian OCs cultured on bone and double-stained for ricin and NaPi-2 protein (NH$_2$ terminus); *C* shows that the OC in *B* was positioned on a resorption pit; (*D*) Immunostaining for NaPi-2 and (*E*) ricin, separately. (*F*) *xz* scan of the dual-label immunofluorescence for ricin and NaPi- 2, with the arrows pointing toward either the basolateral membrane or the apical surface (facing bone) of the OC.
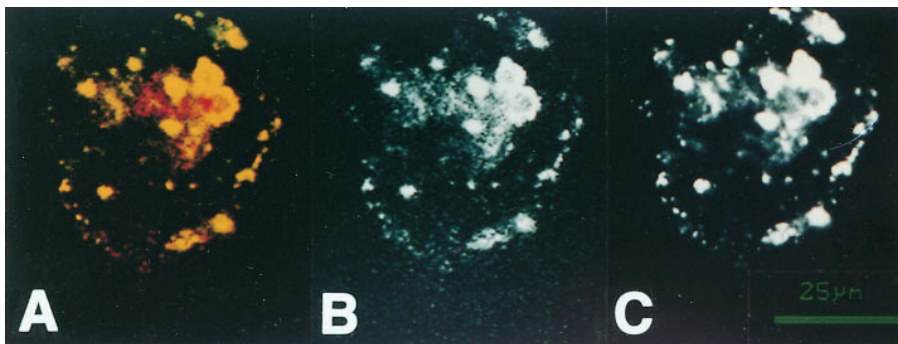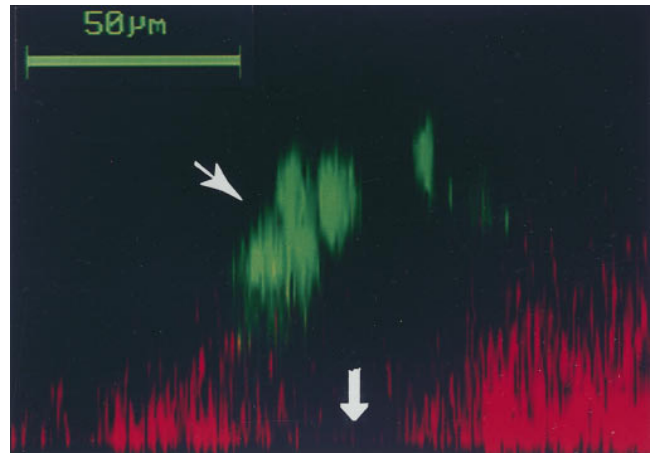

Figure 5. Localization of NaPi-2 protein in endosomes in rabbit OCs using laser scanning confocal microscopy. (*A*) Apical images of rabbit OCs cultured on glass and double-stained with both TRITC-conjugated ricin and the NaPi-2 antibody (NH$_2$ terminus). (*B*) Corresponding immunolocalization of NaPi-2, and (*C*) ricin, separately.

Figure 7. Basolateral location of NaPi in the polarized rabbit OC. Rabbit OCs were cultured on bone and immunostained with the NaPi-2 antibody (NH$_2$ terminus). An *xz* scan of OC stained for the NaPi (FITC); the top arrow points to the basolateral membrane of the OC, whereas the resorption pit is indicated by the bottom arrow facing downward.

*Figure 6.* Double-label immunofluorescence for NaPi-2 and H-ATP-ase in the avian OC. Chicken OCs were cultured on bone and immunostained with the NaPi-2 antibody (NH$_2$ terminus) and the antibody E-11 for the H-ATPase. (*A*) Series of basolateral-to-apical scans (4 μm steps) of the avian OC dual stained for both NaPi-2 (FITC) and H-ATPase (Texas red). There is a high degree of colocalization of the two proteins only on the basolateral surface of the OC (pseudocolored yellow). As the bone surface is approached, the immunostaining is distinctly different for the two proteins toward the center of the cell which actually faces a resorption cavity. (*B*) An apical image of the OC ∼ 5 μm from the surface of bone and the resorption cavity as shown in *A*. This representative focal plane shows the immunostaining pattern for both the H-ATPase and NaPi-2. (*C*) An *xz* image of the OC representing the immunostaining for NaPi-2 on the basolateral membrane of the OC. (*D*) An *xz* image of the OC representing the immunostaining for H-ATPase; the staining is intense on the membrane facing the resorption cavity. (*E*) Colocalization of both H-ATPase and NaPi-2 only on the basolateral membrane of the OC (pseudocolored yellow).

tured on glass and double-stained for ricin (TRITC) and NaPi (FITC). There is an almost complete absence of peripheral plasma membrane staining, as indicated by the arrows. Discrete endosomes demonstrating colocalization of the toxin and NaPi (yellow) were observed in the cytoplasm. An additional pool of NaPi alone (green) is diffusely distributed. OCs cultured on glass are not polarized, but upon attachment to bone they reorganize into highly polarized cells. An OC cultured on bone and double-labeled for ricin and NaPi is shown in Fig. 4 *B*. The pattern of colocalization is very different from that on
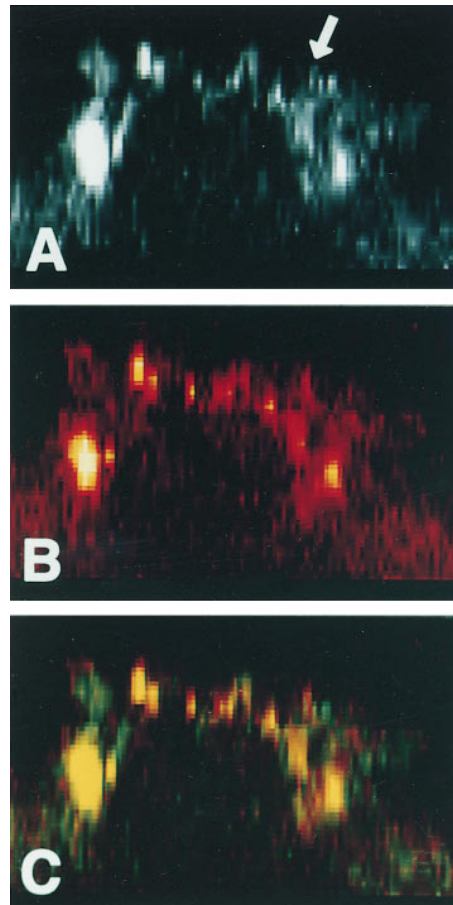
Figure 8. Colocalization of NaPi with the Na-H exchanger (NHE-1 isoform) on the basolateral membrane of avian OCs on bone. Chicken OCs were cultured on bone and immunostained with the NaPi-2 antibody (NH$_2$ terminus) and antibody 4E9 for NHE-1. (*A*) An *xz* scan of OC stained for the NaPi (FITC); the arrow points to the basolateral membrane of the OC. (*B*) An *xz* scan of OC stained for NHE-1 (TRITC). (*C*) Colocalization of NHE-1 with the NaPi on basolateral membrane, especially at the clear zone area of adhesion, as indicated by pseudocolored yellow.

glass with areas of intense staining on the plasma membrane. The OC shown in Fig. 4 *B* was positioned on a resorption pit as shown in Fig. 4 *C*. Fig. 4, *D* and *E*, shows the separate staining patterns for NaPi and ricin, respectively, taken from the cellular sections just above the resorption pit. Fig. 4 *F* shows the *xz* (cross section) scan for colocalization of ricin and NaPi-2; the intensity of staining is greatest at the basolateral membrane of the polarized OC. Identical results to those in Fig. 4 were obtained using rabbit OCs cultured on glass, as shown in Fig. 5. Fig. 5 *A* shows the endosomal colocalization of ricin and the NaPi, whereas the individual staining patterns for ricin and the NaPi are shown in Fig. 5, *B* and *C*, respectively. There is both a peripheral and an intracellular distribution of the endosomal compartment in the unpolarized rabbit OC.

Distribution of NaPi in polarized OCs. To further examine the cellular distribution of the NaPi, the distribution of another membrane transporter, the vacuolar H-ATPase, was investigated. The H-ATPase is known to distribute preferentially, but not completely, toward the ruffled membrane of the polarized OC (2). Fig. 6 *A* shows a series of basolateral (top of the cell) to apical (bottom of the cell facing substrate) scans (4 μm) of a chicken OC on bone double-labeled for both NaPi-2 (NH_2-terminal antibody) and H-ATPase (E11). There is colocalization of the two proteins only on the basolateral surface of the OC (yellow); however, as the bone surface is approached, the immunofluorescence is distinctly different for the two proteins toward the center of the cell which actually faces a resorption cavity. The staining pattern for H-ATPase (red) localized at the cell surface facing the resorption cavity, presumably the ruffled membrane, while the NaPi was limited to the basolateral membrane. The sections obtained in Fig. 6 *A* were used to generate corresponding *xz* scans as shown in *C*. *B* shows the dual immunofluorescent labeling for NaPi-2 and H-ATPase, at ∼ 5 μm from the bone surface. The *xz* image of the OC taken from lines in *B* demonstrates significant colocalization for the two proteins on the basolateral membrane of the OC whereas the H-ATPase is located both on the basolateral and the ruffled membrane.

Similar to that of the chicken OC, the NaPi is also basolaterally located in the polarized rabbit OC, as shown in Fig. 7. Rabbit OCs were cultured on dentine slices before they were processed for immunostaining. A rabbit OC is shown positioned on top of a resorption pit. The basolateral location of the NaPi (in FITC) is readily apparent, whereas the bone surface is represented by red, as visualized by reflection microscopy.

We have shown previously that the NHE-1 isoform of the Na/H exchanger is localized on the basolateral membrane of the polarized OC (14). Similarly, as shown in Fig. 8, the NaPi (*A*) and the Na/H exchanger (*B*) manifest a high degree of colocalization (*C*) only on the basolateral membrane of avian OCs. There was no apparent staining for either of the two proteins on the apical membrane facing the bone surface.

Phosphate uptake by the avian OC: stimulation by bone. Because the immunolocalization data suggest traffic of an endosomal compartment containing NaPi-2–like OC protein to the plasma membrane during organization of the OC in the presence of bone, we questioned whether the stimulation of Pi uptake by bone could be mediated by integrin-signaling mechanisms which stimulate OC polarization for resorption. We have shown previously that the stimulation of Pi uptake by bone could be attenuated by preincubating OCs with Arg-Gly-

Asp-Ser–containing peptides but not by cycloheximide or actinomycin D (10). The Arg-Gly-Asp-Ser–peptides were presumed to compete with integrin-binding sites on OCs cultured in the presence of bone. A probable candidate signaling molecule in the regulation of Pi uptake in OCs, phosphatidylinositol 3-kinase (PI 3-K) activity, has been implicated in the regulation of the basal plasma membrane glucose transporter (GLUT4). PI 3-K participates in insulin-stimulated recycling and reorganization of the intracellular transporter pools of GLUT4 both in adipose tissue and skeletal muscle (21, 22). Furthermore, we have shown that PI 3-K activity in OCs is stimulated via integrin-mediated signaling (23), and its inhibition blocks bone resorption. When used at low concentrations (≤ 100 nM), wortmannin has been shown to be a relatively specific inhibitor of PI 3-K (24). Avian OC precursors allowed to differentiate in 24-well plates for 5 d were exposed to bone particles (+Bone, 600 μg/ml) 4 h before the initiation of Pi uptake, in the presence of wortmannin (100 nM) which was added to cells 30 min before initiation of Pi uptake. As shown in Fig. 9, there was a significant stimulation of Pi uptake in the presence of bone (917.6±44.86 nmol/mg protein at 60 min, $P < 0.01$) compared to that in the absence of bone (248.3±9.33 nmol/mg protein). However, there was an ∼ 50% reduction in Pi uptake (224.2±116.80 nmol/mg protein, $P < 0.01$) in cells pretreated with wortmannin compared to Pi uptake in the presence of bone alone.

Since PI 3-K regulates actin cytoskeletal reorganization during motility and attachment to bone, we also questioned whether disruption of the actin cytoskeleton by cytochalasin D (25) or the microtubular network by colchicine (26) would inhibit Pi uptake by OCs stimulated by bone. As shown in Fig. 10, cytochalasin D (5 ng/ml) inhibited the stimulation of Pi uptake in the presence of bone (81.3±16.81 μmol/mg protein at 60 min, $n = 9$) by ∼ 78% (10.1±2.03, $n = 6$). Colchicine (100 μM), which disrupts microtubules and inhibits bone resorption
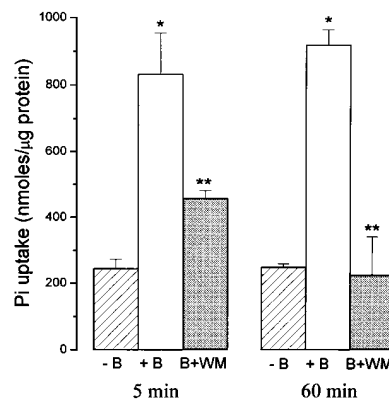
Figure 9. Effects of wortmannin on bone-mediated stimulation of Pi uptake in avian OCs. Avian OC precursors were allowed to differentiate into mature OCs in culture for 5 d. These OCs were exposed to bone particles (+*B*, 600 μg/ml) 4 h before the initiation of Pi uptake, either in the absence or presence of wortmannin (*B*+*WM*, 100 nM). OCs which were not exposed to either bone nor wortmannin served as the untreated controls (−*B*). 100 nM wortmannin was added to cells 30 min before initiation of Pi uptake. Na-dependent Pi uptake was initiated with 1 μCi/ml of $K_2[^{32}P]$-HPO_4 in the assay buffer (see Methods); uptake was measured at both 5 and 60 min. Pi uptake was terminated by washing the cells twice in ice-cold PBS and then solubilizing them with 250 μl of 0.2 N NaOH. The samples were processed for liquid scintillation counting and protein determination. Pi uptake is represented as means±SEM in nmol/μg protein ($n = 3$). Background uptake of ^{32}Pi in the absence of Na was subtracted in each condition.
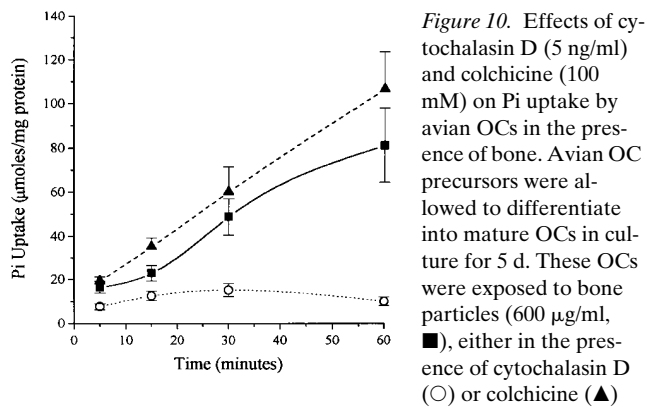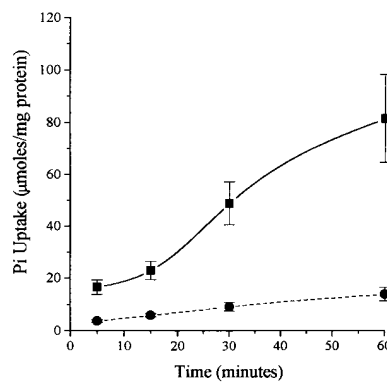
Figure 10. Effects of cytochalasin D (5 ng/ml) and colchicine (100 mM) on Pi uptake by avian OCs in the presence of bone. Avian OC precursors were allowed to differentiate into mature OCs in culture for 5 d. These OCs were exposed to bone particles (600 μg/ml, ■), either in the presence of cytochalasin D (○) or colchicine (▲) 4 h before the initiation of the Pi uptake assay. Na-dependent Pi uptake was initiated with 1 μCi/ml of $K_2[^{32}P]HPO_4$ in the assay buffer for 5, 15, 30, and 60 min. Pi uptake was terminated by washing the cells twice in ice-cold PBS and then solubilizing them with 250 μl of 0.2 N NaOH. These samples were processed for liquid scintillation counting and protein determination. Pi uptake is represented as means±SEM in μmol/mg protein ($n = 6$–9 determinations). Background uptake of ^{32}Pi in the absence of Na was subtracted in each experimental condition.
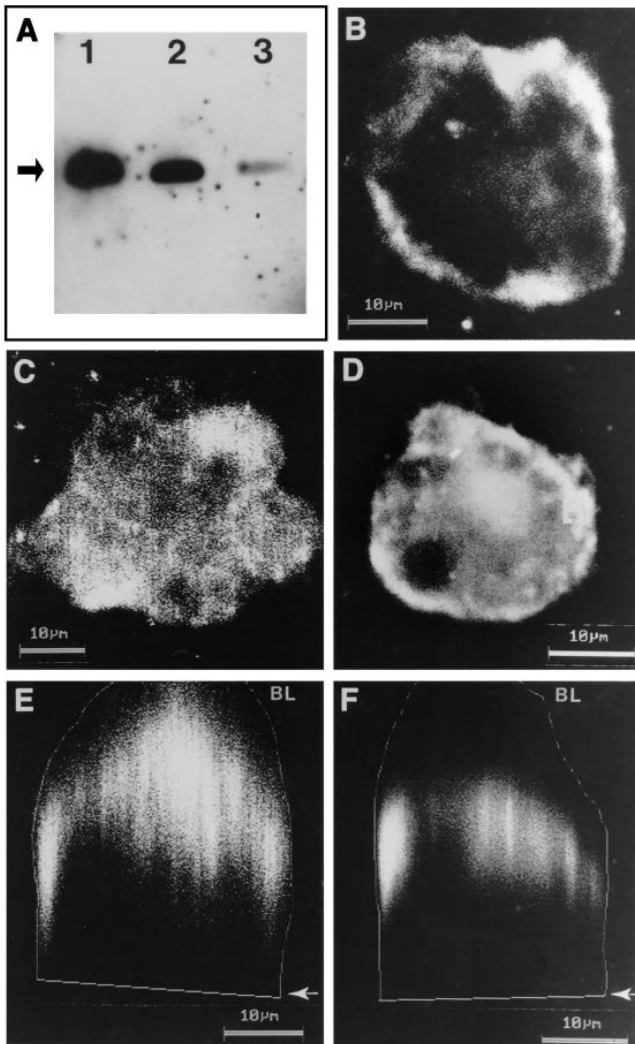

Figure 11. Time course of Pi uptake by avian OCs: effects of PFA in the presence of bone. Avian OC precursors were allowed to differentiate into mature OCs in culture for 5 d. These OCs were exposed to either bone particles alone (600 μg/ml, ■) or a combination of bone and PFA (5 mM, ●), 4 h before the initiation of the Pi uptake assay. Na-dependent Pi uptake was initiated with 1 μCi/ml of $K_2[^{32}P]HPO_4$ in the assay buffer for 5, 15, 30, and 60 min. Pi uptake was terminated by washing the cells twice in ice-cold PBS and then solubilizing them with 250 μl of 0.2 N NaOH. These samples were processed for liquid scintillation counting and protein determination. Pi uptake is represented as means±SEM in μmol/mg protein ($n = 3$).

(27), had no inhibitory effect on Pi uptake in the presence of bone (106.7±16.9 μmol/mg protein, $n = 6$).

The effect of PFA on OC Pi transport. Since exposure to bone markedly increased Pi uptake, we questioned whether PFA, a specific inhibitor of the renal NaPi (28), could also inhibit Pi uptake by the OC. PFA is known to exert its inhibitory effect by binding to the same locus where both Pi and Na$^+$ form a ternary complex with the NaPi. Pi uptake was initiated after a 4-h exposure to bone particles (600 μg/ml) in the presence and absence of PFA (5 mM). As shown in Fig. 11, PFA treatment produced ∼ 70% inhibition of Pi uptake at 60 min (13.8±2.61 μmol/mg protein, $n = 3$) compared to that in the presence of bone alone (81.3±16.81 μmol/mg protein, $n = 9$, $P < 0.001$). To provide an indication of the specificity of PFA on Pi transport in the bone, we examined the effects of PFA on Na-dependent Pi uptake in osteoblast-like cells. We have been unable to find evidence for an NaPi-2–like protein in osteoblasts, either by immunologic cross-reactivity or by detection of message using PCR. We have observed in osteoblast-like UMR-106-01 cells that although the presence of bone increased Na-dependent Pi uptake PFA did not inhibit Pi transport (data not shown). Since the NaPi proteins are the PFA binding proteins (28, 29), the effect of PFA on OC Pi transport is additional evidence of an NaPi-like protein in the OC.

We next determined whether the inhibition of NaPi activity by both PFA and wortmannin was accompanied by a corresponding loss of its expression at the cell surface. We performed two separate sets of experiments which comprised both immunolocalization and cell surface biotinylation of the NaPi in the OC. For the biotinylation studies, avian OCs were cultured in the presence of bone particles for 48 h in the presence of either 5 mM PFA or 100 nM wortmannin (1-h pretreatment). Untreated OCs cultured in the presence of bone particles served as the controls. As shown in Fig. 12 *A*, the levels of the biotinylated NaPi are not affected greatly by treatment with PFA (lane *2*) compared to that in controls (lane *1*). However, when OCs were pretreated with wortmannin (100

nM) for 1 h before the addition of bone particles, there was a dramatic reduction in the levels of the NaPi at the cell surface (lane *3*). For the immunolocalization studies of the NaPi under corresponding conditions, avian OCs were cultured on bone wafers for 3 d, after being pretreated for 1–2 h with 5 mM PFA or 100 nM wortmannin. Fig. 12, *B–D*, shows the corresponding confocal immunofluorescent studies for both the untreated (control), PFA-, and wortmannin-treated OCs. As shown in *B*, there was a significant level of NaPi expression at the periphery of the untreated OC on bone with little intracellular staining. However, when the cells were treated with PFA (5 mM), the intensity of the intracellular staining for the NaPi was greatly increased (*C*), although a decrease in cell surface staining is not readily apparent, as suggested by the biotinylation studies. In addition, as shown in *D*, in OCs pretreated with 100 nM wortmannin, there was an even greater increase in the diffuse intracellular staining than seen with PFA. Therefore, we obtained the corresponding *xz* scans for the control (*B*) and the wortmannin-treated group of OCs (*D*). As shown in *E*, the staining for the NaPi is very close to the basolateral domain of the OC; the cell periphery is outlined in free hand. In contrast, the staining pattern for NaPi in the wortmannin-treated OC is distinctly intracellular with very little basolateral staining.

The effect of NaPi transport inhibition on bone resorption. We had initially hypothesized that the NaPi is recruited to the plasma membrane for Pi uptake during bone resorption in order to provide the Pi for energy metabolism (30). We next asked the question whether inhibition of Pi uptake could attenuate the capacity of the OC to resorb bone. Fig. 13 shows the results of a quantitative bone resorption assay to assess the effects of PFA on bone resorption by OCs, represented as cpm [^{3}H]proline/mg protein (percentage of control). OC precursors were allowed to differentiate in the presence of [^{3}H]proline-labeled bone (2.5×10^5 cpm/well) in 24-well plates. On day 3, varying doses of 1, 2, and 5 mM PFA were added to each well. On day 5, 1.0 ml of the culture media was sampled for [^{3}H]proline release (cpm [^{3}H]proline/mg protein). On day 6, the medium was sampled again, then the cells were lysed with 0.2 N NaOH to assay for protein content. The dose-dependent inhibitory effects of PFA on bone resorption (expressed as per-
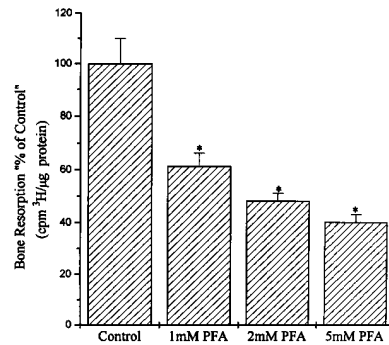
Figure 13. Dose-dependent inhibition of OC-mediated bone resorption by PFA: release of ³H-prelabeled proline. Avian OC precursors were allowed to differentiate into mature OCs in culture in the presence of bone chips (600 µg/ml) for 5 d in 24-well plates. On day 1, ³H-bone chips (2.5×10^5 cpm/well) were added. On day 3, PFA was added at various concentrations of 1, 2, and 5 mM to each well. Untreated cultures served as the controls. 1.0 ml of the culture media was sampled from each of the different treatment groups on both days 4 and 5 to assess the amount of ³H-bone being resorbed. After the last sampling period, the cells were lysed with 0.2 N NaOH and assayed for protein content. Bone resorption is represented as percentage of control (cpm ³H/mg protein).

teologic discs (Millenium Biologix Inc.), which are quartz plates coated with a 1-µm-thick film of calcium phosphate. This system provides a very reliable estimation of bone resorption (17). As shown in Fig. 15 *A*, there was extensive dissolution of the calcium phosphate film by untreated control OCs, manifested by dark spots on the osteologic disc. In contrast, there was a dramatic reduction in the extent of bone resorption by OCs treated with 1, 2.5, and 5 mM PFA (Fig. 15, *B–D*). The higher magnification (×20) images in Fig. 15, *E–H* show the corresponding resorption pits: the extensive resorption by the untreated control group of OCs is apparent (*E*) whereas minimal resorption is seen in the PFA-treated groups (*F–H*). The re-

Figure 12. Effects of PFA and wortmannin on cell surface expression of NaPi. (*A*) Biotinylation of NaPi. Avian OCs were cultured in 24-well plates in the absence or presence of bone chips. Biotinylation was performed using sulfo-NHS-biotin (0.5 mg/ml) under the following conditions: +bone (lane *1*), +PFA +bone (lane *2*), and +wortmannin +bone (lane *3*). (*B–D*) Immunolocalization of NaPi. Avian OCs were cultured on dentine slices and were treated with either 5 mM PFA (*C*) or 100 nM wortmannin (*D*). Untreated OCs served as controls (*B*). *E* and *F* show the corresponding *xz* scans for the control OC on bone (*B*) and the wortmannin-treated OC (*D*). The cell periphery of the corresponding OCs were sketched free-hand as they sat on the bone surface.

Figure 14. Inhibition of mouse OC-mediated bone resorption by PFA: release of ³H-prelabeled proline. Mouse OCs were cultured in the presence of bone chips (600 µg/ml) for 5 d in 24-well plates. On day 1, ³H-bone chips (2.5×10^5 cpm/well) were added. On day 3, PFA was added at a concentration of 5 mM to each well. Untreated cultures served as the controls. 1.0 ml of the culture media was sampled from both the control and treated groups on both days 4 and 5 to assess the amount of ³H-bone being resorbed. After the last sampling period, the cells were lysed with 0.2 N NaOH and assayed for protein content. Bone resorption is represented by cpm ³H/mg protein (percentage of control).

centage of control) were apparent at 1 mM (61.3 ± 5.10, $n = 24$), 2 mM (48.2 ± 2.90, $n = 24$), and 5 mM PFA (40.2 ± 2.84, $n = 24$) compared to the control (untreated) group of OCs (100.0 ± 9.91, $n = 24$). We have extended these findings of inhibition of bone resorption by PFA to a mouse OC–stromal cell coculture system (13). Similar to our observations in the avian OC, there was an ~ 50% reduction in bone resorption, as shown in Fig. 14.
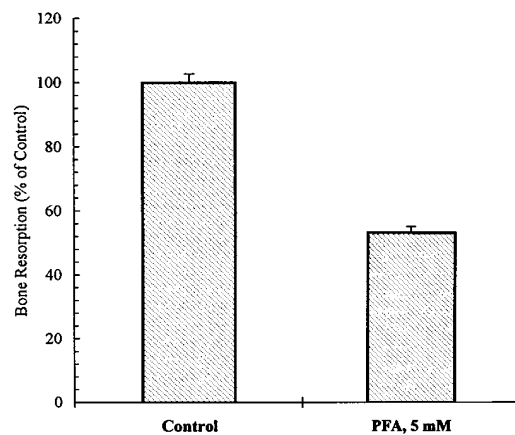
Our observations on the PFA-mediated inhibition of bone resorption by OCs using the release of [³H]proline were corroborated using the pit assay. Avian OCs were cultured on os-
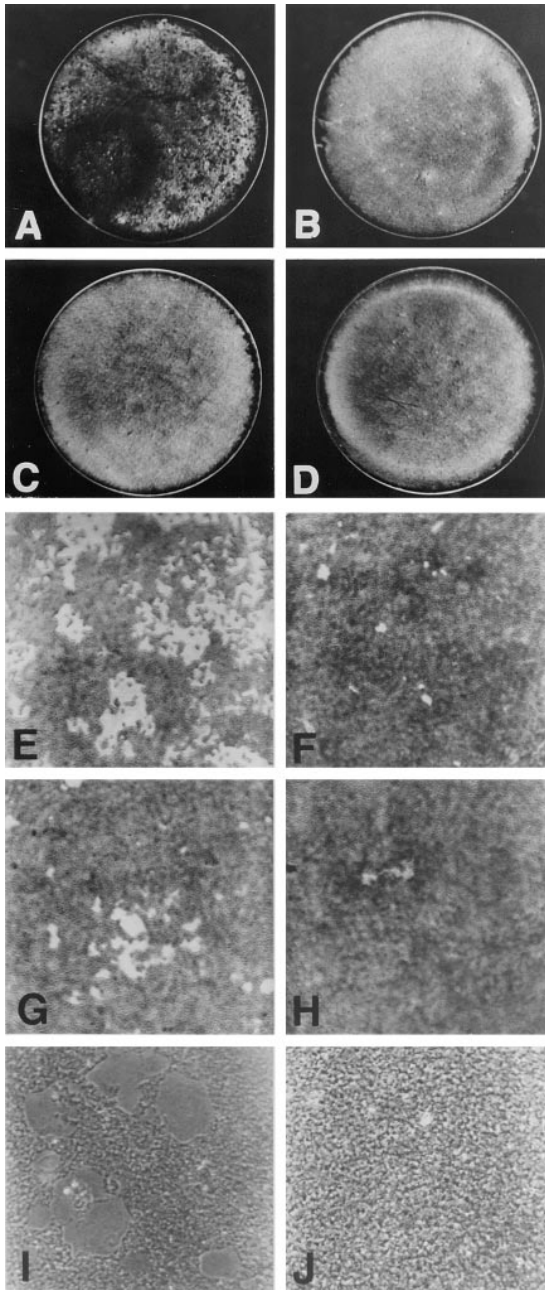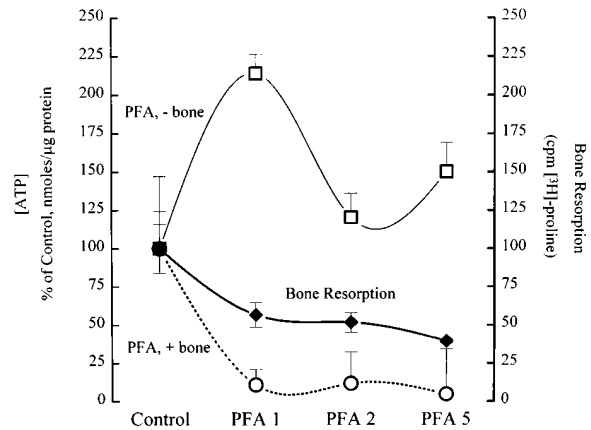
Figure 15. Dose-dependent inhibition of OC-mediated bone resorption by PFA: pit assay. Avian OCs were plated on osteologic discs (coated with a 1-μm-thick calcium phosphate film). These were then cultured for 5 d in 24-well plates. (*A*) Untreated cultures served as the controls. (*B–D*) PFA was added at various concentrations of 1, 2.5, and 5 mM to each well. (*E–H*) ×20 of resorption pits in control, 1, 2.5, and 5 mM PFA-treated cultures. (*I–J*) ×40 of resorption pits in control and 5 mM PFA-treated OCs, respectively.

Figure 16. Effects of PFA on OC-mediated bone resorption and ATP content in avian OCs. Avian OC precursors were allowed to differentiate into mature OCs in culture in 24-well plates. On day 4 in culture, [³H]proline-labeled bone chips (2.5×10^5 cpm/well) were added to two of the cultures. PFA was added at various concentrations of 1, 2, and 5 mM to each well. Untreated cultures served as the controls (100%). ATP content was assayed either in the absence (□) or presence of bone (○). Bone resorption (represented as percentage of control, (◆) was assayed by the OC-mediated release of [³H]proline into the media, as shown on the right axis.

resorption. Our working hypothesis was based upon the premise that limitations of substrate availability in the form of Pi would impair oxidative metabolism (30) in OCs actively resorbing bone. For these experiments, chicken OC precursors were allowed to differentiate (into mature multinucleated OCs) over 4 d in 24-well plates. Three parallel cultures were assayed for the effects of varying doses of PFA (1, 2, and 5 mM) on ATP content in OCs and bone resorption. After 48 h in the absence and presence of bone ([³H]proline-labeled bone particles), an ATP assay was performed on the cultures. As shown in Fig. 16, the addition of PFA to OCs actively resorbing bone led to a dose-dependent decline in bone resorption ($39.6 \pm 1.25\%$ of maximal at 5 mM, $n = 3$), expressed as percentage of control (100.0 ± 16.10, $n = 3$). As shown in Fig. 15, there was no apparent effect from varying doses of PFA on ATP content ([ATP]) in OCs cultured in the absence of bone (PFA, − bone). The ATP content was unchanged from $100 \pm 24.33\%$ (control) to $150 \pm 19.17\%$ (5 mM PFA). This indicated that the OCs were not adversely affected by chronic exposure to PFA (over 48 h) and that a possible lack of cell viability was not a contributing factor in the inhibition of bone resorption by PFA. However, when the OCs were exposed to PFA in the presence of bone, there was a significant reduction of cell ATP content from $100 \pm 47.22\%$ ($n = 3$) in control/untreated OCs to ∼5% ($n = 3$), maximal at 5 mM PFA.

Discussion

In this study, we demonstrate that antibodies directed either toward the COOH- and/or the NH₂-terminal portions of the renal NaPi-2 cross-react with an ∼95-kD protein in both avian and rabbit OCs. By PCR, we show the presence of an NaPi-6–related cDNA sequence in a rabbit OC library. We also demonstrate that a chemical agent, PFA, which binds to and inhibits the renal NaPi proteins, inhibits OC but not osteoblast Pi

sorption pits made by the control group of OCs on the osteologic discs can be seen in more detail in a ×40 image (*I*), in contrast to the total absence of resorptive activity in the PFA-treated OC (*J*). Therefore, our data suggest that avian OC-mediated bone resorption is acutely sensitive to PFA, with an apparent threshold of ∼1 mM.

We next proposed to determine whether PFA was able to inhibit oxidative metabolism in OCs actively engaged in bone

transport in the presence of bone. PFA, however, does not alter expression levels of the NaPi on the cell surface, as judged from our biotinylation studies. This result is in agreement with the possibility that PFA is a competitive inhibitor of the transport protein, as studies in the kidney indicate (28). The first conclusion of this study is that the OC 95-kD protein is related to the renal NaPi-2 to -6 cotransporters. The basis for the larger than expected apparent molecular size is unknown, but one possibility is that the OC NaPi is an alternate splice variant of the renal NaPi family. Glycosylation does not appear to be the basis for the difference in apparent molecular size as the OC 95-kD protein is insensitive to endoglycosidases, in contrast to that reported previously for NaPi-2 (19).

Immunolocalization studies of the OC using the NaPi-2 (NH_2 and COOH termini) antibodies reveal the presences of a cross-reactive protein in discrete vesicles and unpolarized OC cultured on glass which redistributed toward the periphery of cells exposed to bone matrix. Na-dependent Pi transport in the OC was stimulated in the presence of bone, associated with the stimulation of the NaPi-like protein expression in the plasma membrane. Vesicular cytoplasmic immunostaining for the NaPi in unpolarized OCs suggests the presence of an intracellular pool of NaPi (31, 32). Immunofluorescence data demonstrating colocalization of the NaPi and ricin, a general marker for endocytosis and recycling of internalized membrane proteins (20), further support the endosomal nature of the vesicular pools containing the NaPi. Upon attachment to bone, dual immunofluorescence microscopy revealed that the NaPi and NHE-1 localize to the basolateral domain of the polarized OC, in contrast to the vacuolar H-ATPase which sorts to the ruffled membrane facing the bone surface. Therefore, we have demonstrated that bone stimulates insertion or targeting of the NaPi to the basolateral membrane. The expression of a transport protein for uptake of Pi in the basolateral membrane of the OC may seem surprising. However, it is known that the NaPi transports monobasic $H_2PO_4^-$ less effectively than $HPO_4^=$ in renal and intestinal epithelia (33). Therefore, the ambient pH of the resorption space would render an NaPi-2–like protein comparatively inefficient, since protons compete with Na^+ for binding to the external Na^+ interaction site. Thus, the basolaterally located protein would be exposed to an ambient pH closer to its maximum efficiency.

The mechanisms accounting for movement of the NaPi-containing vesicular compartment to the plasma membrane remain to be investigated. However, our observations demonstrating inhibition of both bone-stimulated Pi uptake and surface expression of the NaPi by wortmannin suggest that PI 3-K may be linked to regulation of Pi transport in the OC. It is possible that wortmannin may inhibit general vesicular traffic or inhibit other molecule/components which are critical to Pi uptake. Our preliminary results are reminiscent of the involvement of PI 3-K in the insulin-induced stimulation of GLUT4-containing vesicles translocating to the plasma membrane in adipose tissue and skeletal muscle in response to insulin (22). Our biotinylation studies suggest that the cell surface expression levels of the NaPi are reduced in the presence of wortmannin. Furthermore, cytochalasin D, which promotes actin disassembly, inhibited the stimulation of NaPi in the presence of bone, linking previous studies of the OC actin cytoskeleton and PI 3-K (23) to bone-stimulated traffic of the NaPi-like transporter. Previous studies have shown that cytochalasin D inhibits formation of the ruffled border and consequently bone

resorption (25). However, the microtubule-disrupting agent colchicine had no effect on OC Pi uptake although it, too, has been reported to disrupt the OC ruffled border (26, 27). We have corroborated the latter observations of inhibition of bone resorption by both cytochalasin D and colchicine. When the OC becomes polarized in the presence of bone, it forms three distinct membranes: a ruffled membrane, a sealing zone facing the bone substrate, and a basolateral membrane (1). Our data suggest that during this polarization, there may be an associated redistribution of NaPi to the basolateral membrane of the OC.

The vesicular cytoplasmic immunostaining for the NaPi in unpolarized chicken OCs suggests the presence of an intracellular pool of NaPis (31, 32). Our immunofluorescence data demonstrate that discrete vesicles stain for the NaPi and for TRITC-conjugated ricin. Since ricin is used as a general marker for endocytosis and recycling of apically internalized membrane proteins (20), our double-label immunofluorescence demonstrates a high degree of colocalization of the OC NaPi-2 protein and ricin in these endosomal pools.

Our dual immunofluorescence microscopy for the NaPi, the H-ATPase, and the Na/H exchanger attest to the specificity of the basolateral location of the transporter. The expression of a transport protein for uptake of Pi in the basolateral membrane of the OC may seem surprising. It is known that the NaPi transports monobasic $H_2PO_4^-$ less effectively than $HPO_4^=$ in renal and intestinal epithelia (33). Therefore, the ambient pH of the resorption space would render an NaPi-2–like protein comparatively inefficient, since protons compete with Na^+ for binding to the external Na^{2+} interaction site. However, in contrast to the renal and intestinal epithelia, Na-dependent Pi uptake is higher at pH 6.5 compared to pH 7.4 in ROS 17/2.8 osteoblast-like cells (34, 35), which suggested that the monobasic form of Pi, $H_2PO_4^-$, was the preferred substrate. The stimulatory effect of low pH on Pi uptake in osteoblasts is characteristic of the type III family of NaPis shown to be present in the osteoblast (9). We have yet to determine the preferred substrate for the Na-dependent Pi uptake in OCs.

PFA was originally discovered to be a specific, competitive and reversible inhibitor of NaPi-transport across the brush-border membrane of the renal proximal tubule (28). Our data on inhibition of Pi uptake by PFA ($\sim$ 80% at 5 mM) in OCs are compatible with previous studies in the kidney. The observation that PFA inhibits bone resorption raises several interesting possibilities. Native human OCs have a high capacity to generate ATP via the Krebs cycle, and this is increased during the process of bone resorption (3). OCs are also biosynthetic cells (1) but when they encounter bone or initiate resorption, the normal levels of biosynthesis requiring de novo RNA production are diminished, partly due to the generation of free radicals (36). OCs use high rates of β-fatty acid oxidation to support generation of Krebs cycle intermediates (37), and limitations of a substrate such as Pi could limit ATP generation (7, 8). Our functional and immunochemical results show that in the absence of bone, the OC's NaPi are not expressed at the surface to any great extent. Only when the OC becomes polarized does its capacity to transport Pi increase. Therefore, the OC may become limited in Pi availability (resulting in ATP depletion) in the presence of PFA. We have corroborated the latter hypothesis by testing the effects of PFA on ATP content in OCs in the absence and presence of bone. In the absence of bone, the energy requirements of OCs are minimal since they are not engaged in bone resorption. In this quiescent situation,

the NaPi is not expressed to any significant degree on the plasma membrane. The lack of effect of PFA on OC ATP content demonstrates that the drug was not toxic to the OCs.

The increased surface expression and activity of the NaPi in the polarized bone-resorbing OC would serve to drive Pi uptake from the interstitial fluid after its release from the dissolution of bone, in order to maintain its energy requirements. Therefore, in summary, OCs cultured in the presence of bone particles exhibit an increase in the level of the NaPi in both the microsomal and plasma membrane fractions. This upregulation may reflect the acute increases in Pi uptake observed in the presence of bone. Inhibition of Pi uptake in the presence of bone blocks bone resorption, demonstrating the importance of phosphate transport in the process.

Acknowledgments

References

1. Baron, R., J.H. Ravesloot, L. Neff, M. Chakraborty, D. Chatterjee, A. Lomri, and W. Horne. 1993. Cellular and molecular biology of the osteoclast. *In* Cellular and Molecular Biology of Bone. M. Noda, editor. Academic Press Inc., New York. 445–495.

2. Blair, H.C., S.L. Teitelbaum, R. Ghiselli, and S. Gluck. 1989. Osteoclastic bone resorption by a polarized vacuolar proton pump. *Nature (Lond.).* 245:855–857.

3. Bradbeer, J.N., M. Gowen, and R.A. Dodds. 1992. In situ demonstration of the increased ability of human osteoclasts to generate ATP during bone resorption. *J. Bone Miner. Res.* 7:S312.

4. Magagnin, S., A. Werner, D. Markovich, V. Sorribas, G. Stange, J. Biber, and H. Murer. 1993. Expression cloning of human and rat renal cortex Na/P$_i$ cotransport. *Proc. Natl. Acad. Sci. USA.* 90:5979–5983.

5. Verri, T., D. Markovich, C. Perego, F. Norbis, G. Stange, V. Sorribas, J. Biber, and H. Murer. 1995. Cloning of a rabbit renal NaPi cotransporter which is regulated by dietary phosphate. *Am. J. Physiol.* 268:F626–F633.

6. Werner, A., M.L. Moore, N. Mantei, J. Biber, G. Semenza, and H. Murer. 1991. Cloning and expression of cDNA for a Na/Pi cotransport system of kidney cortex. *Proc. Natl. Acad. Sci. USA.* 88:9608–9612.

7. Werner, A., H. Murer, and R.K.H. Kinne. 1994. Cloning and expression of a renal NaPi cotransport system from flounder. *Am. J. Physiol.* 267:F311–F317.

8. Custer, M., M. Lötscher, J. Biber, H. Murer, and B. Kaissling. 1994. Expression of NaPi cotransport in rat kidney: localization by RT-PCR and immunohistochemistry. *Am. J. Physiol.* 266:F767–F774.

9. Kavanaugh, M.P., and D. Kabat. 1996. Identification and characterization of a widely expressed phosphate transporter/retrovirus receptor family. *Kidney Int.* 49:959–963.

10. Gupta, A., A. Miyauchi, A. Fujimori, and K.A. Hruska. 1996. Phosphate transport in osteoclasts: a functional and immunochemical characterization. *Kidney Int.* 49:968–974.

11. Alvarez, J.I., S.L. Teitelbaum, H.D. Blair, E.M. Greenfield, N.A. Athanasou, and F.P. Ross. 1991. Generation of avian cells resembling osteoclasts from mononuclear phagocytes. *Endocrinology.* 128:2324–2325.

12. Tezuka, K., Y. Tezuka, A. Maejima, T. Sato, K. Nemoto, H. Kamioka, Y. Hakeda, and M. Kumegawa. 1994. Molecular cloning of a possible cysteine proteinase predominantly expressed in osteoclasts. *J. Biol. Chem.* 269:1106–1109.

13. Shioi, A., F.P. Ross, and S.L. Teitelbaum. 1994. Enrichment of generated murine osteoclasts. *Calcif. Tissue Int.* 55:387–394.

14. Gupta, A., J.C. Edwards, and K.A. Hruska. 1996. Cellular distribution and regulation of NHE-1 isoform of the Na-H exchanger in the avian osteoclast. *Bone (N.Y.).* 18:87–95.

15. Sambrook, J., E.F. Fritsch, and T. Maniatis. 1989. Molecular Cloning: A Laboratory Manual, 2nd Ed. Cold Spring Harbor Laboratory Press, Cold Spring Harbor, NY.

16. Sanger, F.A., S. Nicklen, and A.R. Coulson. 1977. DNA sequencing with chain-terminating inhibitors. *Proc. Natl. Acad. Sci. USA.* 74:5463–5467.

17. Nakamura, I., N. Takahashi, T. Sasaki, E. Jimi, T. Kurokawa, and T. Suda. 1996. Chemical and physical properties of the extracellular matrix are required for the actin ring formation in osteoclasts. *J. Bone Miner. Res.* 11:1873–1879.

18. Adams, H. 1963. Methods in Enzymatic Analysis. H.U. Bergmeyer, editor. Academic Press Inc., NY. 539–543.

19. Hayes, G., A. Busch, M. Lotscher, S. Waldegger, F. Lang, F. Verrey, J. Biber, and H. Murer. 1984. Role of N-linked glycosylation in rat renal Na/Pi-cotransport. *J. Biol. Chem.* 269:24143–24149.

20. van Deurs, B., S.H. Hansen, O.W. Petersen, E.L. Melby, and K. Sandvig. 1990. Endocytosis, intracellular transport and transcytosis of the toxic protein ricin by a polarized epithelium. *Eur. J. Cell Biol.* 51:96–109.

21. Cheatham, B., C. Vlahos, L. Cheatham, L. Wang, J. Blenis, and C.R. Kahn. 1994. Phosphatidylinositol 3-kinase activation is required for insulin stimulation of pp70 S6 kinase, DNA synthesis, and glucose transporter translocation. *Mol. Cell. Biol.* 14:4902–4911.

22. Okada, T., L. Sakuma, Y. Fukui, O. Hazeki, and M. Ui. 1994. Essential role of phosphatidylinositol 3-kinase in insulin-induced glucose transport and antilipolysis in rat adipocytes. *J. Biol. Chem.* 269:3563–3567.

23. Hruska, K.A., F. Rolnick, M. Huskey, U. Alvarez, and D.A. Cheresh. 1995. Engagement of the osteoclast integrin $\alpha_v\beta_3$ by osteopontin stimulates phosphatidylinositol 3-hydroxyl kinase activity. *Endocrinology.* 136:2984–2992.

24. Thelen, M., M.P. Wymann, and H. Langen. 1994. Wortmannin binds specifically to 1-phosphatidylinositol 3-kinase while inhibiting guanine nucleotide-binding protein-coupled receptor signaling in neutrophil leukocytes. *Proc. Natl. Acad. Sci. USA.* 91:4960–4964.

25. Sasaki, T., K. Debari, and N. Udagawa. 1993. Cytochalasin D reduces osteoclastic bone resorption by inhibiting development of ruffled border-clear zone complex. *Calcif. Tissue Int.* 53:217–221.

26. Borisy, G.G., and E.W. Taylor. 1967. The mechanism of action of colchicine. Binding of colchicine-^{3}H to cellular protein. *J. Cell Biol.* 34:525–533.

27. Rowe, D.J., and E. Hausmann. 1980. The effects of calcitonin and colchicine on the cellular response to diphosphonate. *Br. J. Exp. Pathol.* 61:303–309.

28. Yusufi, A.N.K., M. Szczepanska-Konkel, S.A. Kempson, J.A. McAteer, and T.P. Dousa. 1986. Inhibition of human renal epithelial Na$^+$/Pi cotransport by phosphonoformic acid. *Biochem. Biophys. Res. Commun.* 139:679–686.

29. Szczepanska-Konkel, M., A.N.K. Yusufi, M. VanScoy, S.K. Webster, and T.P. Dousa. 1986. Interactions of [^{14}C]phosphonoformic acid with renal cortical brush-border membranes. *J. Biol. Chem.* 261:6375–6383.

30. Brazy, P.C., L.J. Mandel, S.R. Gullans, and S.P. Soltoff. 1984. Interactions between phosphate and oxidative metabolism in proximal renal tubule. *Am. J. Physiol.* 247:F575–F581.

31. Biber, J., M. Custer, A. Werner, B. Kaissling, and H. Murer. 1993. Localization of NaPi-1, a Na/Pi cotransporter, in rabbit kidney proximal tubules. II. Localization by immunohistochemistry. *Pflueg. Arch. Euro. J. Physiol.* 424:210–215.

32. Loghman-Adham, M., G.T. Motock, P. Wilson, and M. Levi. 1995. Characterization of Na$^+$-phosphate cotransporters in renal cortical endosomes. *Am. J. Physiol.* 268:F93–F102.

33. Ullrich, K.J., and H. Murer. 1982. Sulphate and phosphate transport in the renal proximal tubule. *Philos. Trans. R. Soc. Lond. B Biol. Sci.* 299:549–558.

34. Selz, T., J. Caverzasio, and J.P. Bonjour. 1989. Regulation of Na-dependent Pi transport by parathyroid hormone in osteoblast-like cells. *Am. J. Physiol.* 256:E93–E100.

35. Caverzasio, J., T. Selz, and J.P. Bonjour. 1988. Characteristics of phosphate transport in osteoblast-like cells. *Calcif. Tissue Int.* 48:83–87.

36. Garrett, I.R., B.F. Boyce, R.O.C. Oreffo, L. Bonewalde, J. Poser, and G.R. Mundy. 1990. Oxygen-derived free radicals stimulate osteoclastic bone resorption in rodent bone in vitro and in vivo. *J. Clin. Invest.* 85:632–639.

37. Dodds, R.A., M. Gowen, and J.N. Bradbeer. 1994. Microcytophotometric analysis of human OC metabolism: lack of activity in certain oxidative pathways indicates inability to sustain biosynthesis during resorption. *J. Histochem. Cytochem.* 42:599–606.